Frontiers of Information Technology & Electronic Engineering
www.jzus.zju.edu.cn; engineering.cae.cn; www.springerlink.com
ISSN 2095-9184 (print); ISSN 2095-9230 (online)
E-mail: jzus@zju.edu.cn

Practical fixed-time adaptive fuzzy control of uncertain nonlinear systems with time-varying asymmetric constraints: a unified barrier function based approach*

Zixuan HUANG†‡[1], Huanqing WANG[2], Ben NIU[3], Xudong ZHAO[4], Adil M. AHMAD[5]

[1]*College of Engineering, Bohai University, Jinzhou 121013, China*

[2]*College of Mathematical Science, Bohai University, Jinzhou 121013, China*

[3]*School of Information Science and Engineering, Shandong Normal University, Jinan 250014, China*

[4]*Faculty of Electronic Information and Engineering, Dalian University of Technology, Dalian 116024, China*

[5]*Communication Systems and Networks Research Group, Department of Information Technology, Faculty of Computing and Information Technology, King Abdulaziz University, Jeddah, Saudi Arabia*

†E-mail: huangzixuan0301@163.com

Received June 8, 2023; Revision accepted Oct. 13, 2023; Crosschecked Aug. 28, 2024

Abstract: A practical fixed-time adaptive fuzzy control strategy is investigated for uncertain nonlinear systems with time-varying asymmetric constraints and input quantization. To overcome the difficulties of designing controllers under the state constraints, a unified barrier function approach is employed to construct a coordinate transformation that maps the original constrained system to an equivalent unconstrained one, thus relaxing the time-varying asymmetric constraints upon system states and avoiding the feasibility check condition typically required in the traditional barrier Lyapunov function based control approach. Meanwhile, the "explosion of complexity" problem in the traditional backstepping approach arising from repeatedly derivatives of virtual controllers is solved by using the command filter method. It is verified via the fixed-time Lyapunov stability criterion that the system output can track a desired signal within a small error range in a predetermined time, and that all system states remain in the constraint range. Finally, two simulation examples are offered to demonstrate the effectiveness of the proposed strategy.

Key words: Unified barrier function; Time-varying asymmetric state constraints; Fuzzy logic systems; Fixed-time control; Command filter

https://doi.org/10.1631/FITEE.2300408 **CLC number:** TP13

1 Introduction

Over the past few decades, uncertain nonlinear systems that provide a unified mathematical description for most practical systems have received considerable attention from many researchers. Adaptive backstepping technique (Ma et al., 2019; Sun et al., 2021; Zhang et al., 2021), a powerful controller design tool for nonlinear systems, combined with some powerful function approximators (e.g., neural networks or fuzzy logic systems, FLSs for short), has been extensively applied to address tracking or the regulation problem for many categories of nonlinear systems, including single-input and single-output nonlinear systems (Wang HQ et al., 2013; Wang T et al., 2015), multiple-input and multiple-output nonlinear systems (Chen B et al., 2013), and large-scale nonlinear systems (Chen WS and Li, 2010). Note that

‡ Corresponding author

* Project supported by Institutional Fund Projects (No. IFPIP: 131-611-1443)

ORCID: Zixuan HUANG, https://orcid.org/0009-0000-5508-1475

one disadvantage neglected in current backstepping-based control schemes is the "explosion of complexity" issue, resulting from repeated differentiations of virtual control signals in the design procedure. To address this issue, Swaroop et al. (2000) initially presented an adaptive dynamic surface control scheme for strict-feedback nonlinear systems, where a first-order filter was introduced to mitigate the expansion of differential terms of intermediate signals. Following Swaroop et al. (2000), some modified control strategies free from the issue of "explosion of complexity" have been researched for uncertain nonlinear systems (Yang et al., 2016; Li YM and Tong, 2017; Sui and Tong, 2018). However, these control schemes were proposed under the framework of asymptotic stability; in other words, they only ensure that a system is stable when time tends to infinity, which may limit their application in some practical systems.

As is well known, finite-time control (Bhat and Bernstein, 1998) is one of the most effective approaches for rapidly realizing the control goal. In comparison with asymptotic stability, finite-time control has a higher convergence rate, shorter response time, and greater anti-disturbance. Thanks to these advantages, finite-time control has been extensively employed in many real systems, such as robotic manipulator systems (Yu et al., 2005), servo motor systems (Hou et al., 2020), and autonomous underwater vehicle systems (Li SH and Wang, 2013). It should be mentioned that, in the above finite-time control strategies, the settling time of systems is influenced by the initial system values, which causes the settling time to be inaccurately calculated. To achieve an exact settling time, a so-called fixed-time control lemma was first presented in Polyakov (2012), in which the settling time was entirely unrelated to the initial condition, and its upper bound can be calculated using theoretical methods. Following Polyakov (2012), many schemes based on fixed-time control have been proposed. Li JP et al. (2017) developed a fixed-time backstepping control approach and obtained a semi-globally fixed-time convergence system property. In Ni et al. (2017), a fast fixed-time sliding mode control approach was developed for power systems, which restrained chaotic system oscillations. Given the new practical fixed-time stability criterion, Wang F and Lai (2020) offered a new scheme to realize fixed-time control of uncertain strict-feedback nonlinear systems. Compared with the traditional fixed-time stability criteria in Polyakov (2012), Li JP et al. (2017), and Ni et al. (2017), the one in Wang F and Lai (2020) relaxes the limitations of the sufficient condition and extends the applied range of fixed-time control. Note that the above fixed-time control schemes are suitable only for nonlinear systems whose states are unconstrained, which motivates our current research.

In actual engineering, constraints resulting from physical limitations or safety requirements are frequently encountered, e.g., maximum and minimum chemical reactor temperatures and joint active space for a robotic arm. During system operation, violating some constraint conditions may lead to system performance degradation or instability, which requires that system states must remain within constrained ranges. To resolve the constraints, a barrier Lyapunov function (BLF) approach was first presented in Tee et al. (2009), and many significant results have been obtained (Tee and Ge, 2011; Kim and Yoo, 2015; Liu YJ and Tong, 2017; Huang S et al., 2023; Liu SL et al., 2024), in which the Lyapunov candidate function can be selected as different barrier function forms, such as logarithmic-type BLFs (Liu YJ and Tong, 2017), integral-type BLFs (Kim and Yoo, 2015), and tangent-type BLFs (Zhao H et al., 2023). Actually, as indicated in Tee and Ge (2011) and Tang et al. (2016), only if we search for a series of design parameters satisfying a specific condition, will the BLF-based schemes be available in practice. This restriction is also expressed as the feasibility condition of virtual control signals; namely, the variation range of virtual control signals must stay within certain pre-given constraint areas (Tee and Ge, 2011), which results in difficulties in some controller designs. If the system state constraint range is small, it is likely that the desired control objective will not be achieved (namely, parameters to meet the feasibility condition do not exist). Recently, another way to address the state constraints is the unified barrier function (UBF) approach developed in Zhao K et al. (2020), in which a scalar function was constructed to achieve an equivalent unconstrained model mapped by the original constrained systems; adaptive control of the systems can be realized based on this model. Unlike current BLF-based methods, the proposed UBF-based method in Zhao K et al. (2020) not only effectively relaxes the constraints upon system states, but also

completely removes the feasibility conditions of virtual control signals. It is evident that the UBF-based method has greater application value and development potential than the BLF-based approach. For nonlinear systems with asymmetric state constraints, Wang SX et al. (2021) investigated an adaptive event-triggered control strategy that does not include feasibility conditions using the UBF method to handle the state constraints. Subsequently, in Gao et al. (2022), the UBF approach was extended to interconnected nonlinear systems with dynamic state constraints. On the other hand, communication resource limits for control signal transmissions should be considered during the design process, which can prevent the loss of available information. Shi et al. (2020) constructed a hysteresis quantizer, which reduced the communication burden by generating the input signal within a limited set and had an extra quantification level to alleviate the high-frequency chattering in other quantizers. As far as we know, for systems with state constraints and communication resource limitations, how to make the output of the system track the desired signal at a predetermined time without violating the state constraints is still a meaningful problem in the control field.

Enlightened by the aforementioned discussions, a UBF-based practical fixed-time adaptive fuzzy control approach is proposed in this article for uncertain nonlinear systems with input quantization and time-varying asymmetric constraints. In comparison with existing results, the primary differences and contributions of this research are summarized as the following three points:

1. The proposed control approach can ensure the practical fixed-time stability of a class of uncertain nonlinear systems, while the settling time of the system is entirely unrelated to the initial values of system states and its upper bound can also be obtained.

2. Different from BLF-based schemes (Tee and Ge, 2011; Tang et al., 2016; Li YX, 2020), a new UBF method is used to overcome the difficulties caused by state constraints for designing controllers. This function constructs an unconstrained system model of the original constrained system, so the restrictions on system states are relaxed and the feasibility conditions of virtual control signals are completely eliminated.

3. A modified hysteretic quantizer is constructed to save communication resources in practical applications, and has extra quantization levels to alleviate the high-frequency chatter.

Notations: $\mathbb{R}$ denotes the compact set of real numbers. $\mathbb{R}_+$ represents the compact set of positive real numbers. $\mathbb{R}^j$ expresses the j-dimensional Euclidean space. U_i and U_{d} stand for the constrained region of system state x_i and desired signal y_{d}, respectively. Θ indicates the mathematical set. x^{T} means the transpose of vector x. $|\cdot|$ is the absolute value. $\|\cdot\|$ signifies the standard 2-form. $\Xi_{i\mathrm{l}}$ and $\Xi_{i\mathrm{h}}$ are the compact sets of constraint functions $k_{i\mathrm{l}}(t)$ and $k_{i\mathrm{h}}(t)$, respectively.

2 Problem formulation and preliminaries

2.1 System descriptions and lemmas

Take the following uncertain nonlinear systems into account:

$$\begin{cases} \dot{x}_i = x_{i+1} + f_i\left(\bar{x}_n\right), i = 1, 2, \ldots, n-1, \\ \dot{x}_n = g\left(\bar{x}_n\right) q\left(u\right) + f_n\left(\bar{x}_n\right), \\ y = x_1, \end{cases} \tag{1}$$

where $\bar{x}_n = [x_1, x_2, \ldots, x_n]^{\mathrm{T}} \in \mathbb{R}^n$ denotes the system state vector, y and $q(u)$ indicate the system output and the quantized input, respectively, and $g(\bar{x}_n)$ and $f(\bar{x}_n)$ are the unknown nonlinear functions. In addition, system state x_i is restricted by the time-varying asymmetric constraint, described as follows:

$$\begin{aligned} x_i \in U_i := \big\{(t, x_i) \in (\mathbb{R}_+ \times \mathbb{R}) | \\ k_{i\mathrm{l}}\left(t\right) < x_i < k_{i\mathrm{h}}\left(t\right), k_{i\mathrm{l}} \in \mathbb{R}, k_{i\mathrm{h}} \in \mathbb{R}\big\}. \end{aligned} \tag{2}$$

Remark 1 $k_{i\mathrm{l}}(t)$ and $k_{i\mathrm{h}}(t)$ are first-order differentiable functions defined in set $\Theta := \big\{k_{i\mathrm{l}}(t)\colon \mathbb{R}_+ \to \mathbb{R}, k_{i\mathrm{h}}(t)\colon \mathbb{R}_+ \to \mathbb{R}\big\}$, and their initial conditions are $k_{i\mathrm{l}}(0)$ and $k_{i\mathrm{h}}(0)$, respectively, satisfying $k_{i\mathrm{l}}(0) \in \Xi_{i\mathrm{l}}$ and $k_{i\mathrm{h}}(0) \in \Xi_{i\mathrm{h}}$. Also, $k_{i\mathrm{l}}(t)$ and $k_{i\mathrm{h}}(t)$ have the relationship $k_{i\mathrm{l}}(t) < k_{i\mathrm{h}}(t)$.

The hysteresis quantizer is shown as follows:

$$q(u) = \begin{cases} u_i \mathrm{sgn}(u), & \frac{u_i}{1+\delta} < |u| \le u_i, \dot{u} < 0 \text{ or} \\ & u_i < |u| \le \frac{u_i}{1-\delta}, \dot{u} > 0, \\ u_i(1+\delta), & u_i < |u| \le \frac{u_i}{1-\delta}, \dot{u} < 0 \text{ or} \\ & \frac{u_i}{1-\delta} < |u| \le \frac{u_i(1+\delta)}{1-\delta}, \dot{u} > 0, \\ 0, & 0 \le |u| < \frac{u_{\min}}{1+\delta}, \dot{u} < 0 \text{ or} \\ & \frac{u_{\min}}{1+\delta} \le u \le u_{\min}, \dot{u} > 0, \\ q(u(t^-)), & \text{otherwise}, \end{cases} \tag{3}$$

where $\delta=\frac{1-\lambda}{1+\lambda}$ and $u_i=\lambda^{1-i}u_{\min}$ $(i=1,2,...)$, with $u_{\min}>0$ deciding the range of the dead zone for $q(u)$. The parameter λ satisfying $0<\lambda<1$ denotes the measure of quantization density. Fig. 1 displays the map of hysteresis quantizer (3). According to Guo et al. (2023), the quantized input can be disassembled as two parts, namely, $q(u)=G(u)u+D(t)$, where $0<1-\delta\le G(u)\le 1+\delta$ and $|D(t)|\le u_{\min}$.

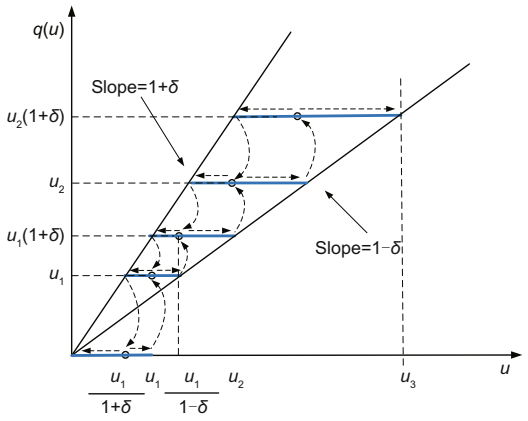

Fig. 1 Map of hysteresis quantizer $q(u)$

Remark 2 The hysteresis quantizer can be classified as a non-uniform quantizer owing to its unequal quantization level. This quantizer is the coarsest quantizer, which minimizes the average speed of communication cases and is simple to realize in practice. Different from other quantizers, the hysteresis quantizer has extra quantization levels to mitigate undesired chattering.

The control goal of this paper is to design a practical fixed-time adaptive controller for the considered system (1), which makes the system output y follow the desired signal $y_{\rm d}$ and all states remain within the time-varying asymmetric state constraints. To achieve this goal, we give some common assumptions and lemmas as follows:

Assumption 1 The function $g(\bar{x}_n)$ is unknown and bounded, and there exist positive constants $\bar{g}$ and $\underline{g}$ which make the inequality $0<\underline{g}\le g(\bar{x}_n)\le\bar{g}<\infty$ hold.

Assumption 2 The desired signal $y_{\rm d}$ is defined in set $U_{\rm d}:=\{(t,y_{\rm d})\in[0,\infty)\times\mathbb{R}: k_{\rm dl}(t)\le y_{\rm d}\le k_{\rm dh}(t)\}$, and its derivatives up to the second order are bounded and known. Meanwhile, there exist positive constants $\bar{\xi}$ and $\underline{\xi}$ such that inequalities $k_{1\rm h}(t)-k_{\rm dh}(t)\ge\bar{\xi}>0$ and $k_{\rm dl}(t)-k_{1\rm l}(t)\ge\underline{\xi}>0$ hold (i.e., $U_{\rm d}\subset U_1$).

Remark 3 Assumption 1 indicates the boundedness of control gain functions, and it is reasonable to require that $g(\bar{x}_n)$ is away from zero to make the system controllable. Moreover, in practical cases, the control gain is not always a constant.

Lemma 1 (Wang F and Lai, 2020) For a nonlinear system, if there exists a positive definite function $V(x)$ that satisfies

$$\begin{cases}\dot{V}(x)\le -c_1V^p(x)-c_2V^q(x)+b,\\ \beta(\|x\|)\le V(x)\le\alpha(\|x\|),\end{cases}\tag{4}$$

where $c_1,c_2>0$, $q>1$, $0<p<1$, $0<b<\min\{(1-\xi)c_1,(1-\xi)c_2\}$ $(0<\xi<1)$, and α, β are κ_∞-functions, then we can deduce that the system is practically fixed-time stable, and the upper bound of the settling time $T_{\rm s}$ can be computed by $T\le T_{\rm s}=\frac{1}{\xi c_1(1-p)}+\frac{1}{\xi c_2(q-1)}$.

Lemma 2 (Li YX, 2019) For real variables x,s and arbitrary positive constants a, b, ω, there exists $|s|^a|x|^b\le\frac{a}{a+b}\omega|s|^{a+b}+\frac{b}{a+b}\omega^{-\frac{a}{b}}|x|^{a+b}$.

Lemma 3 (Zuo et al., 2018) Suppose that variable $s_i\ge0$ and two positive constants $0<r<1$, $m>1$. Then we can deduce $\left(\sum_{i=1}^{n}s_i\right)^r\le\sum_{i=1}^{n}s_i^r$ and $\left(\sum_{i=1}^{n}s_i\right)^m\le n^{m-1}\sum_{i=1}^{n}s_i^m$.

Lemma 4 (Huang JS et al., 2018) If the positive definite function $V(t)$ satisfies $V(t)\le\sum_{j=1}^{n}\int_0^t\big(k_j(N_j(v_j)-1)\dot{v}_j(\tau)\big)\mathrm{d}\tau+c$, where $N_j(v_j)$ is a Nussbaum-type function and c, k_j are positive constants, then we can infer that $V(t)$, $\sum_{j=1}^{n}\int_0^t(k_j(N_j(v_j)-1)\dot{v}_j(\tau))\mathrm{d}\tau$, and v_j are bounded.

Lemma 5 (Xu et al., 2022) Assume that $s\ge0$ is a real number. We have $s\le s^n+s^m$, where $0<n<1$ and $m>1$ are constants.

2.2 Fuzzy logic systems

As we know, FLSs can approximate the unknown nonlinear function to arbitrary accuracy. According to Zhao H et al. (2023), the unknown nonlinear function $f(X)$ can be represented as $f(X)=W^{\rm T}S(X)+\delta(X)$, where $X\in\mathbb{R}^m$ indicates the input vector and $W=[w_1,\ w_2,\ ...,\ w_l]^{\rm T}$ represents the optimal weight vector. $\delta(X)$ expresses the approximation error and satisfies $|\delta|\le\varepsilon$ with ε being a positive constant. $S(X)=[\zeta_1(X),\zeta_2(X),...,\zeta_l(X)]^{\rm T}$ indicates the basis function vector, and $\zeta_i(X)$ is chosen

as a Gaussian function, described as

$$\zeta_i(X)=\exp\left(-\frac{(X-\mu_i)^{\mathrm{T}}(X-\mu_i)}{\sigma^2}\right),\ 1\le i\le l, \quad (5)$$

where l expresses the number of fuzzy rules, $\mu_i=[\mu_{i1},\mu_{i2},...,\mu_{im}]^{\mathrm{T}}$ denotes the center vector, and σ stands for the width of the Gaussian function.

2.3 Unified barrier function

In this subsection, we will present some properties of the UBF. The definition of the UBF is as follows:

Definition 1 (UBF) (Zhao K et al., 2020) The scalar function $\zeta(x)$ is a UBF, if the scalar function $\zeta(x)$ $(x\in U)$ satisfies the following conditions:

1. The state constraints are disposed without modifying the function structure.

2. It shows a performance that $\zeta\to\pm\infty$ when x is close to the boundary of U, and there exists a bounded constant c such that $\zeta\le c\ \forall x\in U^{'}\subset U$ under the initial condition $x(0)\in U$, where $U^{'}$ is a closed interval.

Considering Definition 1, by defining $\zeta_{i,1}=\frac{\bar{k}_{i\mathrm{l}}-k_{i\mathrm{l}}+k_{i\mathrm{h}}-\underline{k}_{i\mathrm{h}}}{(x_i-k_{i\mathrm{l}})(k_{i\mathrm{h}}-x_i)}$ and $\zeta_{i,2}=\frac{k_{i\mathrm{l}}\underline{k}_{i\mathrm{h}}-\bar{k}_{i\mathrm{l}}k_{i\mathrm{h}}}{(x_i-k_{i\mathrm{l}})(k_{i\mathrm{h}}-x_i)}$, the UBF of x_i can be constructed as

$$\zeta_i=\zeta_{i,1}x_i+\zeta_{i,2}, \quad (6)$$

where $\bar{k}_{i\mathrm{l}}$ and $\underline{k}_{i\mathrm{h}}$ are constants satisfying $k_{i\mathrm{l}}(t)<\bar{k}_{i\mathrm{l}}$ and $\underline{k}_{i\mathrm{h}}<k_{i\mathrm{h}}(t)$, respectively. Then, constructing $\zeta_{i,3}=\frac{\zeta_{i,2}}{\zeta_{i,1}}$, the system state x_i can be reformulated as

$$x_i=\frac{\zeta_i}{\zeta_{i,1}}-\zeta_{i,3}. \quad (7)$$

In addition, from Zhao K et al. (2020), we can obtain the following property for ζ_i:

$$\begin{cases}\zeta_i\to-\infty \text{ when } x_i\to k_{i\mathrm{l}}^{+}(t),\\ \zeta_i\to+\infty \text{ when } x_i\to k_{i\mathrm{h}}^{-}(t).\end{cases} \quad (8)$$

The constructed UBF ζ_i contributes to creating an unconstrained equivalent model later and preventing system states from violating the time-varying asymmetric constraints. The closed-loop control structure of the controlled system is given in Fig. 2.

3 Main results

In this section, we first need to construct an unconstrained equivalent model for control system (1). Second, based on this model, a practical fixed-time adaptive controller is established by applying FLSs and dynamic surface control methods. Finally, the stability analysis outcomes are offered to verify the stability of the systems.

3.1 Design of an equivalent unconstrained model

In this subsection, to facilitate the subsequent formula derivation, we need to construct an unconstrained equivalent model of the original constrained system. This process is described in the following in detail.

First, taking the derivative of ζ_i produces

$$\dot{\zeta}_i=\eta_{i,1}\dot{x}_i+\eta_{i,2}, \quad (9)$$

where $\eta_{i,1}=\frac{\bar{k}_{i\mathrm{l}}-k_{i\mathrm{l}}}{(x_i-k_{i\mathrm{l}})^2}+\frac{k_{i\mathrm{h}}-\underline{k}_{i\mathrm{h}}}{(k_{i\mathrm{h}}-x_i)^2}$ and $\eta_{i,2}=\frac{(x_i-\bar{k}_{i\mathrm{l}})\dot{k}_{i\mathrm{l}}}{(x_i-k_{i\mathrm{l}})^2}+\frac{\dot{k}_{i\mathrm{h}}(x_i-\underline{k}_{i\mathrm{h}})}{(k_{i\mathrm{h}}-x_i)^2}$. Then, integrating system model (1) with Eq. (9), we can arrive at an equivalent model as follows:

$$\begin{cases}\dot{\zeta}_i=\eta_{i,1}(f_i(\bar{x}_n)+x_{i+1})+\eta_{i,2},\\ \dot{\zeta}_n=\eta_{n,1}(f_n(\bar{x}_n)+gq(u))+\eta_{n,2},\end{cases} \quad (10)$$

where g is short for $g(\bar{x}_n)$.

Substituting Eq. (7) into Eq. (10), the equivalent model becomes

$$\begin{cases}\dot{\zeta}_i=\eta_{i,1}(f_i(\bar{x}_n)+\frac{\zeta_{i+1}}{\zeta_{i+1,1}}-\zeta_{i+1,3})+\eta_{i,2},\\ \dot{\zeta}_n=\eta_{n,1}(f_n(\bar{x}_n)+gq(u))+\eta_{n,2},\end{cases} \quad (11)$$

where ζ_i is the new state variable without state constraints. From this, for any initial condition $x_i(0)\in U_i$, if ζ_i can be made bounded, then state x_i is kept in region U_i; namely, states remain within a pre-determined constraint interval. It should be pointed out that $\zeta_{i,1}$, $\zeta_{i,2}$, $\zeta_{i,3}$, $\eta_{i,1}$, and $\eta_{i,2}$ are well defined in U_i. Here, the unconstrained equivalent model is constructed.

3.2 Controller design

In this subsection, we will apply the backstepping technique to construct the practical fixed-time adaptive controller. The main design procedure can be broken down into n steps, whose details are shown later. To relax the time-varying asymmetric constraint and to eliminate the feasibility condition, a coordinate transformation based on the converted model (11) is introduced

$$e_i=\zeta_i-\alpha_{i,\mathrm{f}},\ i=1,2,...,n, \quad (12)$$

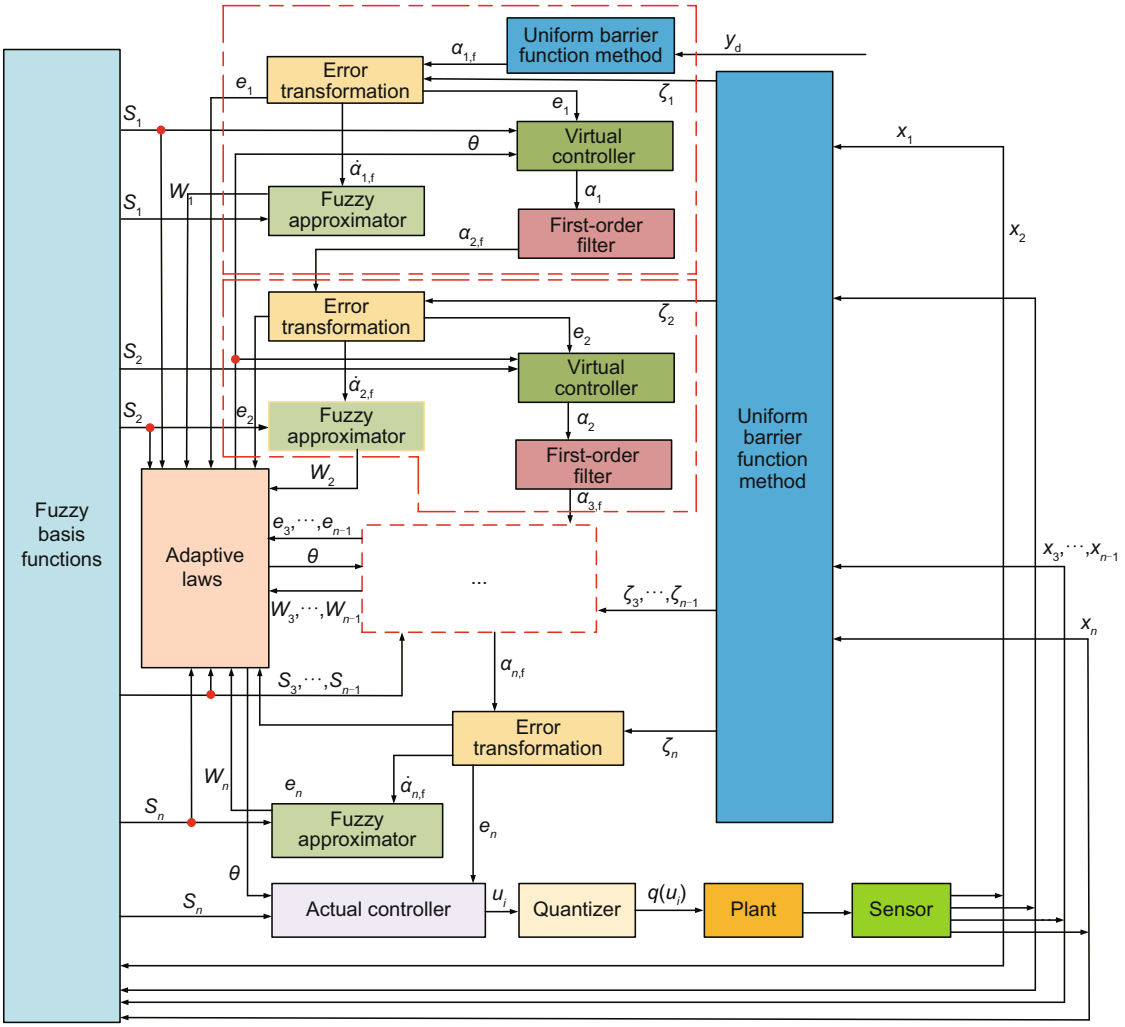

Fig. 2 Closed-loop control structure of the controlled system

where $\alpha_{1,\mathrm{f}} = \frac{y_\mathrm{d}-\bar{k}_{11}}{y_\mathrm{d}-k_{11}} + \frac{y_\mathrm{d}-\underline{k}_{1\mathrm{h}}}{k_{1\mathrm{h}}-y_\mathrm{d}}$, and $\alpha_{i,\mathrm{f}}$ is the output signal of the first-order filter.

Define the first-order filter as

$$\tau_i \dot{\alpha}_{i,\mathrm{f}} + \alpha_{i,\mathrm{f}} = \alpha_{i-1},\ i = 2, 3, ..., n, \tag{13}$$

where $\tau_i > 0$ is a constant, and the virtual control signal α_{i-1} is the input signal of the first-order filter.

Step 1: Establish the Lyapunov candidate function as $V_1 = \frac{1}{2}e_1^2 + \frac{1}{2\gamma}\tilde{\theta}^2$ with $\gamma > 0$ being a design parameter, and calculate the derivative of e_1 using

$$\begin{aligned}\dot{e}_1 = {}& \eta_{1,1}(f_1 + \tfrac{e_2}{\zeta_{2,1}} + \tfrac{\alpha_1}{\zeta_{2,1}} - \zeta_{2,3}) \\ & + \eta_{1,1}(\tfrac{\alpha_{2,\mathrm{f}}}{\zeta_{2,1}} - \tfrac{\alpha_1}{\zeta_{2,1}}) + \eta_{1,2} - \dot{\alpha}_{1,\mathrm{f}}.\end{aligned} \tag{14}$$

Then, taking the derivative of V_1, there exists

$$\begin{aligned}\dot{V}_1 = {}& e_1(\tfrac{\eta_{1,1}}{\zeta_{2,1}}e_2 + \tfrac{\eta_{1,1}}{\zeta_{2,1}}\alpha_1 - \eta_{1,1}\zeta_{2,3} + \eta_{1,2}) \\ & + e_1\tfrac{\eta_{1,1}}{\zeta_{2,1}}e_{2,\alpha} + e_1(\eta_{1,1}f_1 - \dot{\alpha}_{1,\mathrm{f}}) - \tfrac{1}{\gamma}\tilde{\theta}\dot{\hat{\theta}},\end{aligned} \tag{15}$$

where $e_{2,\alpha} = \alpha_{2,\mathrm{f}} - \alpha_1$ denotes the filtering error. Define $h_1(Z_1) = \eta_{1,1}f_1 - \dot{\alpha}_{1,\mathrm{f}}$ with $Z_1 = [\bar{x}_n, \dot{\alpha}_{1,\mathrm{f}}]^\mathrm{T}$ as the input of FLSs. Because $h_1(Z_1)$ includes the unknown uncertainties, it can be expressed within the approximation error $\delta_1(Z_1)$ as FLSs of the following form:

$$h_1(Z_1) = W_1^\mathrm{T}S_1(Z_1) + \delta_1(Z_1), \tag{16}$$

where $||\delta_1(Z_1)|| \le \varepsilon_1$ and $\varepsilon_1 > 0$ is a constant. With the assistance of Young's inequality, there exist

$$\begin{aligned}e_1h_1(Z_1) = {}& e_1(W_1^\mathrm{T}S_1(Z_1) + \delta_1(Z_1)) \\ \le {}& \tfrac{1}{2a_1^2}e_1^2\theta S_1^\mathrm{T}S_1 + \tfrac{1}{2}a_1^2 \\ & + k_1e_1^2 + \tfrac{1}{4k_1}\varepsilon_1^2,\end{aligned} \tag{17}$$

$$\frac{\eta_{1,1}}{\zeta_{2,1}}e_{2,\alpha}e_1 \le \frac{1}{2}e_{2,\alpha}^2 + \frac{1}{2}e_1^2\Big(\frac{\eta_{1,1}}{\zeta_{2,1}}\Big)^2, \tag{18}$$

where $a_1>0$ is a constant, and $\theta=\max\{||W_1||^2, ||W_2||^2, ..., ||W_n||^2\}$ denotes the adaptive parameter.

It can be immediately obtained from (15), (17), and (18) that

$$\begin{aligned}\dot{V}_1 \le\ & e_1(\tfrac{\eta_{1,1}}{\zeta_{2,1}}e_2+\tfrac{\eta_{1,1}}{\zeta_{2,1}}\alpha_1-\eta_{1,1}\zeta_{2,3}+\eta_{1,2})\\ &+\tfrac{1}{2}e_{2,\alpha}^2+\tfrac{1}{2}e_1^2(\tfrac{\eta_{1,1}}{\zeta_{2,1}})^2+\tfrac{1}{2}a_1^2+k_1e_1^2\\ &+\tfrac{1}{2a_1^2}e_1^2\theta S_1^{\mathrm{T}}S_1+\tfrac{1}{4k_1}\varepsilon_1^2-\tfrac{1}{\gamma}\tilde{\theta}\dot{\hat{\theta}},\end{aligned}\tag{19}$$

where $\hat{\theta}$ and $\tilde{\theta}$ are the estimate and estimation error of θ, respectively.

If the virtual control law is constructed as

$$\begin{aligned}\alpha_1=\ & -\tfrac{\zeta_{2,1}}{\eta_{1,1}}k_1e_1-\tfrac{\zeta_{2,1}}{\eta_{1,1}}\eta_{1,2}-\tfrac{\eta_{1,1}}{2\zeta_{2,1}}e_1\\ &-\tfrac{\zeta_{2,1}}{\eta_{1,1}}c_{1,1}e_1^{2p-1}-\tfrac{\zeta_{2,1}}{\eta_{1,1}}c_{1,2}e_1^{2q-1}\\ &-\tfrac{\zeta_{2,1}}{\eta_{1,1}}\tfrac{1}{2a_1^2}e_1\hat{\theta}S_1^{\mathrm{T}}S_1+\zeta_{2,1}\zeta_{2,3},\end{aligned}\tag{20}$$

where $c_{1,1}>0$ and $c_{1,2}>0$ are design parameters, then $\dot{V}_1$ satisfies

$$\begin{aligned}\dot{V}_1\le\ & -c_{1,1}e_1^{2p}-c_{1,2}e_1^{2q}-\tfrac{1}{\gamma}\tilde{\theta}\dot{\hat{\theta}}+\tfrac{\eta_{1,1}}{\zeta_{2,1}}e_1e_2\\ &+\tfrac{1}{2a_1^2}e_1^2\tilde{\theta}S_1^{\mathrm{T}}S_1+\tfrac{1}{2}a_1^2+\tfrac{1}{4k_1}\varepsilon_1^2+\tfrac{1}{2}e_{2,\alpha}^2.\end{aligned}\tag{21}$$

Step i ($2\le i\le n-1$): Choose the i^{th} Lyapunov candidate function as $V_i=V_{i-1}+\frac{1}{2}e_i^2$, and calculate the derivative of e_i as

$$\begin{aligned}\dot{e}_i=\ & \eta_{i,1}(\tfrac{e_{i+1}}{\zeta_{i+1,1}}+\tfrac{e_{i+1,\alpha}}{\zeta_{i+1,1}}+\tfrac{\alpha_i}{\zeta_{i+1,1}}-\zeta_{i+1,3})\\ &+\eta_{i,2}+\eta_{i,1}f_i-\dot{\alpha}_{i,\mathrm{f}}.\end{aligned}\tag{22}$$

Then, taking the time-derivative of V_i results in

$$\begin{aligned}\dot{V}_i=\ & \dot{V}_{i-1}+e_i(\eta_{i,1}f_i-\dot{\alpha}_{i,\mathrm{f}})+e_i(\tfrac{\eta_{i,1}e_{i+1}}{\zeta_{i+1,1}}\\ &+\tfrac{\eta_{i,1}e_{i+1,\alpha}}{\zeta_{i+1,1}}+\tfrac{\eta_{i,1}\alpha_i}{\zeta_{i+1,1}}-\eta_{i,1}\zeta_{i+1,3}+\eta_{i,2}),\end{aligned}\tag{23}$$

where $e_{i+1,\alpha}=\alpha_{i+1,\mathrm{f}}-\alpha_i$ is the filtering error. As with Step 1, we define a function $h_i(Z_i)=\eta_{i,1}f_i-\dot{\alpha}_{i,\mathrm{f}}$, and its input is $Z_i=[\bar{x}_n,\ \dot{\alpha}_{i,\mathrm{f}}]^{\mathrm{T}}$. The function $h_i(Z_i)$ can be approximated by FLSs, which is expressed as $h_i(Z_i)={W_i}^{\mathrm{T}}S_i(Z_i)+\delta_i(Z_i)$ and $||\delta_i(Z_i)||\le\varepsilon_i$. By using Young's inequality, it can be deduced that

$$\begin{aligned}e_ih_i(Z_i)=\ & e_i(W_i^{\mathrm{T}}S_i(Z_i)+\delta_1(Z_i))\\ \le\ & \tfrac{1}{2a_i^2}e_i^2\theta S_i^{\mathrm{T}}S_i+\tfrac{1}{2}a_i^2\\ &+k_ie_i^2+\tfrac{1}{4k_i}\varepsilon_i^2,\end{aligned}\tag{24}$$

$$\frac{\eta_{i,1}}{\zeta_{i+1,1}}e_{i+1,\alpha}e_i\le\frac{1}{2}e_{i+1,\alpha}^2+\frac{1}{2}e_i^2\Big(\frac{\eta_{i,1}}{\zeta_{i+1,1}}\Big)^2,\tag{25}$$

where $a_i>0$ is a constant. Considering (24) and (25), one has

$$\begin{aligned}\dot{V}_i\le\ & \dot{V}_{i-1}+\tfrac{1}{2}a_i^2+\tfrac{1}{4k_i}\varepsilon_i^2+\tfrac{1}{2}e_{i+1,\alpha}^2+k_ie_i^2\\ &+\tfrac{1}{2}e_i^2\big(\tfrac{\eta_{i,1}}{\zeta_{i+1,1}}\big)^2+\tfrac{1}{2a_i^2}e_i^2\theta S_i^{\mathrm{T}}S_i+e_i\big(\eta_{i,2}\\ &+\tfrac{\eta_{i,1}}{\zeta_{i+1,1}}e_{i+1}-\eta_{i,1}\zeta_{i+1,3}+\tfrac{\eta_{i,1}}{\zeta_{i+1,1}}\alpha_i\big).\end{aligned}\tag{26}$$

Establish the virtual control law as

$$\begin{aligned}\alpha_i=\ & -\tfrac{\zeta_{i+1,1}}{\eta_{i,1}}\big(c_{i,1}e_i^{2p-1}+c_{i,2}e_i^{2q-1}+\eta_{i,2}\\ &+\tfrac{\eta_{i-1,1}}{\zeta_{i,1}}e_{i-1}+k_ie_i+\tfrac{1}{2a_i^2}e_i\hat{\theta}S_i^{\mathrm{T}}S_i\big)\\ &-\tfrac{\eta_{i,1}}{2\zeta_{i+1,1}}e_i+\zeta_{i+1,1}\zeta_{i+1,3},\end{aligned}\tag{27}$$

where $c_{i,1}$ and $c_{i,2}$ are positive design parameters. By combining (26) and (27), $\dot{V}_i$ can turn into

$$\begin{aligned}\dot{V}_i\le\ & \dot{V}_{i-1}-c_{i,1}e_i^{2p}-c_{i,2}e_i^{2q}-k_ie_i^2\\ &-\tfrac{1}{2}e_i^2\big(\tfrac{\eta_{i,1}}{\zeta_{i+1,1}}\big)^2+\tfrac{\eta_{i,1}}{\zeta_{i+1,1}}e_ie_{i+1}+\tfrac{1}{2}a_i^2\\ &+\tfrac{1}{4k_i}\varepsilon_i^2+k_ie_i^2+\tfrac{1}{2}e_{i+1,\alpha}^2+\tfrac{1}{2}e_i^2\big(\tfrac{\eta_{i,1}}{\zeta_{i+1,1}}\big)^2\\ &-\tfrac{\eta_{i-1,1}}{\zeta_{i,1}}e_ie_{i-1}+\tfrac{1}{2a_i^2}e_i^2\tilde{\theta}S_i^{\mathrm{T}}S_i\\ \le\ & -\sum_{j=1}^{i}(c_{j,1}e_j^{2p}+c_{j,2}e_j^{2q})+\tfrac{\eta_{i,1}}{\zeta_{i+1,1}}e_ie_{i+1}\\ &-\tfrac{\tilde{\theta}}{\gamma}\Big(\dot{\hat{\theta}}-\sum_{j=1}^{i}\gamma\tfrac{1}{2a_j^2}e_j^2S_j^{\mathrm{T}}S_j\Big)\\ &+\sum_{j=1}^{i}(\tfrac{1}{2}a_j^2+\tfrac{1}{4k_j}\varepsilon_j^2+\tfrac{1}{2}e_{j+1,\alpha}^2).\end{aligned}\tag{28}$$

Step n: In this step, a practical fixed-time adaptive controller will be constructed for the considered system (1). In view of the communication resources of the system, a hysteresis quantizer described by model (3) will be used. Build the n^{th} Lyapunov candidate function as $V_n=V_{n-1}+\frac{1}{2}e_n^2$. Computing the derivative of e_n yields

$$\dot{e}_n=\eta_{n,1}(f_n+gq(u))+\eta_{n,2}-\dot{\alpha}_{n,\mathrm{f}}.\tag{29}$$

As $q(u)=G(u)u+D(t)$, $\dot{e}_n$ can be shown as

$$\begin{aligned}\dot{e}_n=\ & \eta_{n,1}(f_n+gG(u)u)\\ &+\eta_{n,2}-\dot{\alpha}_{n,\mathrm{f}}+\eta_{n,1}gD(t).\end{aligned}\tag{30}$$

Taking the time-derivative of V_n, we arrive at

$$\begin{aligned}\dot{V}_n=\ & \dot{V}_{n-1}+e_n(\eta_{n,1}gG(u)u+\eta_{n,2})\\ &+e_n(\eta_{n,1}f_n-\dot{\alpha}_{n,\mathrm{f}})+e_n\eta_{n,1}gD(t).\end{aligned}\tag{31}$$

Similarly, define the function $h_n(Z_n)=\eta_{n,1}f_n-\dot{\alpha}_{n,\mathrm{f}}$ with the variable $Z_n=[\bar{x}_n,\ \dot{\alpha}_{n,\mathrm{f}}]^{\mathrm{T}}$ being the input signal. The function $h_n(Z_n)$ can be approached by FLSs, which is represented as $h_n(Z_n)=W_n^{\mathrm{T}}S_n(Z_n)+\delta_n(Z_n)$ and $||\delta_n(Z_n)||\le\varepsilon_n$. As in the cases of (24) and (25), the following inequality holds:

$$\begin{aligned}e_nh_n(Z_n)=\ & e_n(W_n^{\mathrm{T}}S_n(Z_n)+\delta_n(Z_n))\\ \le\ & \tfrac{1}{2a_n^2}e_n^2\theta S_n^{\mathrm{T}}S_n+\tfrac{1}{2}a_n^2\\ &+k_ne_n^2+\tfrac{1}{4k_n}\varepsilon_n^2,\end{aligned}\tag{32}$$

where $a_n > 0$ is a positive parameter.

Based on Assumption 1, there exists

$$\eta_{n,1} g D(t) e_n \le \tfrac{1}{2}\eta_{n,1}^2 e_n^2 \bar{g}^2 + \tfrac{1}{2}u_{\min}^2. \tag{33}$$

It is clear from (31)–(33) that

$$\begin{aligned}\dot{V}_n \le{}& \dot{V}_{n-1} + e_n(\eta_{n,1} g G(u) u + \eta_{n,2}) \\ &+\tfrac{1}{2a_n^2} e_n^2 \theta S_n^{\mathrm{T}} S_n + \tfrac{1}{2}a_n^2 + k_n e_n^2 \\ &+\tfrac{1}{4k_n}\varepsilon_n^2 + \tfrac{1}{2}\eta_{n,1}^2 e_n^2 \bar{g}^2 + \tfrac{1}{2}u_{\min}^2.\end{aligned} \tag{34}$$

In light of Assumption 1, the virtual controller is established as

$$\begin{aligned}u = {}& \tfrac{1}{\eta_{n,1}\underline{g}(1-\delta)}(-c_{n,1}e_n^{2p-1} - c_{n,2}e_n^{2q-1} \\ &-\tfrac{\eta_{n-1,1}}{\zeta_{n,1}} e_{n-1} - k_n e_n - \tfrac{1}{2a_n^2} e_n \hat{\theta} S_n^{\mathrm{T}} S_n \\ &-\eta_{n,2} - \tfrac{1}{2}\eta_{n,1}^2 e_n \bar{g}^2).\end{aligned} \tag{35}$$

Considering the relationship $0 < 1-\delta \le G(u) \le 1+\delta$ and Assumption 1, we can deduce the following inequality:

$$\begin{aligned}G(u)u \le {}& \tfrac{1}{\eta_{n,1}\underline{g}}(-c_{n,1}e_n^{2p-1} - c_{n,2}e_n^{2q-1} \\ &-\tfrac{\eta_{n-1,1}}{\zeta_{n,1}} e_{n-1} - \tfrac{1}{2a_n^2} e_n \hat{\theta} S_n^{\mathrm{T}} S_n \\ &-k_n e_n - \eta_{n,2} - \tfrac{1}{2}\eta_{n,1}^2 e_n \bar{g}^2).\end{aligned} \tag{36}$$

Substituting (36) into (34) results in

$$\begin{aligned}\dot{V}_n \le{}& \dot{V}_{n-1} - c_{n,1}e_n^{2p} - c_{n,2}e_n^{2q} - k_n e_n^2 \\ &-\tfrac{\eta_{n-1,1}}{\zeta_{n,1}} e_n e_{n-1} + \tfrac{1}{2a_n^2} v_n^2 \tilde{\theta} S_n^{\mathrm{T}} S_n \\ &+\tfrac{1}{2}a_n^2 + \tfrac{1}{4k_n}\varepsilon_n^2 + k_n e_n^2 + \tfrac{1}{2}u_{\min}^2 \\ \le{}& -\sum_{i=1}^{n}(c_{i,1}e_i^{2p} + c_{i,2}e_i^{2q}) + \sum_{i=2}^{n}\tfrac{1}{2}e_{i,\alpha}^2 \\ &+\sum_{i=1}^{n}(\tfrac{1}{2}a_i^2 + \tfrac{1}{4k_i}\varepsilon_i^2) + \tfrac{1}{2}u_{\min}^2 \\ &-\tfrac{\tilde{\theta}}{\gamma}\Big(\dot{\hat{\theta}} - \sum_{i=1}^{n}\gamma\tfrac{1}{2a_i^2}e_i^2 S_i^{\mathrm{T}} S_i\Big).\end{aligned} \tag{37}$$

By constructing the adaptive law as

$$\dot{\hat{\theta}} = \sum_{i=1}^{n}\gamma\tfrac{1}{2a_i^2}e_i^2 S_i^{\mathrm{T}} S_i - \sigma_1\hat{\theta} - \sigma_2\hat{\theta}^{2q-1}, \tag{38}$$

we have

$$\begin{aligned}\dot{V}_n \le{}& -\sum_{i=1}^{n}(c_{i,1}e_i^{2p} + c_{i,2}e_i^{2q}) \\ &+\tfrac{\sigma_1}{\gamma}\tilde{\theta}\hat{\theta} + \tfrac{\sigma_2}{\gamma}\tilde{\theta}\hat{\theta}^{2q} + b_n,\end{aligned} \tag{39}$$

where $b_n = \sum_{i=1}^{n}(\frac{1}{2}a_i^2 + \frac{1}{4k_i}\varepsilon_i^2) + \sum_{i=2}^{n}\frac{1}{2}e_{i,\alpha}^2 + \frac{1}{2}u_{\min}^2$.

According to Young's inequality and Lemma 3, it can be obtained that

$$\begin{aligned}\tfrac{\sigma_1}{\gamma}\tilde{\theta}\hat{\theta} &= -\tfrac{\sigma_1}{\gamma}\tilde{\theta}^2 + \tfrac{\sigma_1}{\gamma}\tilde{\theta}\theta \\ &\le -\sigma_1(\tfrac{\tilde{\theta}^2}{2\gamma})^p + \sigma_1(1-p)p^{\frac{p}{1-p}} + \tfrac{\sigma_1}{2\gamma}\theta^2.\end{aligned} \tag{40}$$

By applying Lemmas 2 and 3, we can infer

$$\tfrac{\sigma_2}{\gamma}\tilde{\theta}\hat{\theta}^{2q} \le 2^{2q-2}\tfrac{\sigma_2}{\gamma}\tfrac{2q-1}{2q}(\theta^{2q} - \tilde{\theta}^{2q}). \tag{41}$$

Substituting (40) and (41) into (39), $\dot{V}_n$ becomes

$$\begin{aligned}\dot{V}_n \le{}& -\sum_{i=1}^{n}(c_{i,1}e_i^{2p} + c_{i,2}e_i^{2q}) - \sigma_1(\tfrac{\tilde{\theta}^2}{2\gamma})^p \\ &+\sigma_1(1-p)p^{\frac{p}{1-p}} + \tfrac{\sigma_1}{2\gamma}\theta^2 + b_n \\ &+2^{2q-2}\tfrac{\sigma_2}{\gamma}\tfrac{2q-1}{2q}(\theta^{2q} - \tilde{\theta}^{2q}) \\ \le{}& -c_1\sum_{i=1}^{n}(\tfrac{e_i^2}{2})^p - c_2\sum_{i=1}^{n}(\tfrac{e_i^2}{2})^q - \sigma_1(\tfrac{\tilde{\theta}^2}{2\gamma})^p \\ &-2^{2q-2}\sigma_2\tfrac{2q-1}{q}(2\gamma)^{2q-1}(\tfrac{\tilde{\theta}^2}{2\gamma})^q + \underline{b}_n,\end{aligned} \tag{42}$$

where $\underline{b}_n = \sigma_1(1-p)p^{\frac{p}{1-p}} + \frac{\sigma_1}{2\gamma}\theta^2 + 2^{2q-2}\frac{\sigma_2}{\gamma}\frac{2q-1}{2q}\theta^{2q} + b_n$, $c_1 = 2^p\min\{c_{1,1}, c_{2,1}, ..., c_{n,1}\}$, and $\underline{c}_2 = 2^q\cdot\min\{c_{1,2}, c_{2,2}, ..., c_{n,2}\}$. Lemma 3 yields

$$\Big(\sum_{i=1}^{n}\frac{e_i^2}{2} + \frac{\tilde{\theta}^2}{2\gamma}\Big)^p \le \sum_{i=1}^{n}\Big(\frac{e_i^2}{2}\Big)^p + \Big(\frac{\tilde{\theta}^2}{2\gamma}\Big)^p, \tag{43}$$

$$(n+1)^{1-q}\Big(\sum_{i=1}^{n}\frac{e_i^2}{2} + \frac{\tilde{\theta}^2}{2\gamma}\Big)^q \le \sum_{i=1}^{n}\Big(\frac{e_i^2}{2}\Big)^q + \Big(\frac{\tilde{\theta}^2}{2\gamma}\Big)^q. \tag{44}$$

Combining (43) and (44) with (42) leads to

$$\begin{aligned}\dot{V}_n &\le -\underline{c}_1\Big(\sum_{i=1}^{n}\tfrac{e_i^2}{2} + \tfrac{\tilde{\theta}^2}{2\gamma}\Big)^p + \underline{b}_n \\ &\quad -\underline{c}_2(n+1)^{1-q}\Big(\sum_{i=1}^{n}\tfrac{e_i^2}{2} + \tfrac{\tilde{\theta}^2}{2\gamma}\Big)^q \\ &\le -\underline{c}_1 {V_n}^p - \bar{c}_2 {V_n}^q + \underline{b}_n,\end{aligned} \tag{45}$$

where $\underline{c}_1 = \min\{c_1, \sigma\}$ and $\bar{c}_2 = \underline{c}_2(n+1)^{1-q}$ with $\underline{c}_2 = \min\{c_2, 2^{2q-2}\sigma_2\frac{2q-1}{q}(2\gamma)^{2q-1}\}$.

So far, we have accomplished the design process of practical fixed-time adaptive control for uncertain nonlinear system (1).

Remark 4 According to Definition 1 and property (8) of ζ_i, if the function ζ_1 follows the signal $\alpha_{1,\mathrm{f}}$ within a desired error region, then we can deduce that the virtual control signal $\alpha_{i,\mathrm{f}}$ is non-constrained. Thus, compared with BLF-based methods, the feasibility condition of virtual control signals is fully removed.

3.3 Stability analysis

Based on the above derived formulation, the primary results are shown as follows:

Theorem 1 Consider uncertain nonlinear system (1) subject to time-varying asymmetric state constraints (2) and quantized input (3) satisfying Assumptions 1 and 2. By designing the virtual control

signals (20) and (27), the practical fixed-time adaptive controller (35) and the adaptive law (38), we can obtain the following:

1. The boundedness of all signals in the closed-loop system (1) can be achieved.

2. The time-varying asymmetric constraints (2) on system states are not overstepped, and feasibility check is avoided.

3. The output signal will follow the desired signal within a small error interval in a predetermined time T, which can be computed using Lemma 1.

Proof First, for convenience, define $V(s) = V_n\big(e_1, e_2, ..., e_n, \tilde{\theta}\big)$ and $s = \big[e_1, e_2, ..., e_n, \tilde{\theta}\big]$. The process of achieving fixed-time stability of closed-loop systems can be separated into two situations.

Situation 1 If $V(s) > 1$ and $\underline{b}_n$ satisfies $\underline{b}_n < \min\big\{(1-\xi)\underline{c}_1, (1-\xi)\bar{c}_2\big\}$ $(0 < \xi < 1)$, we can deduce the following inequalities:

$$\dot{V}(s) \le -\bar{c}_2 V^q(s) + \underline{b}_n, \tag{46}$$

$$\frac{\underline{b}_n}{(1-\xi)\bar{c}_2} \le 1 \le V(s), \tag{47}$$

$$\underline{b}_n \le (1-\xi)\bar{c}_2 V^q(s). \tag{48}$$

Combining (46) and (48), one has

$$\dot{V}(s) \le -\xi\bar{c}_2 V^q(s), \tag{49}$$

which implies

$$\int_0^t \frac{\dot{V}(s)}{V^q(s)}\mathrm{d}t \le -\xi\int_0^t \bar{c}_2\mathrm{d}t. \tag{50}$$

By calculating (50), one has

$$\frac{1}{1-q}V^{1-q}(s(t)) - \frac{1}{1-q}V^{1-q}(s(0)) \le -\xi\bar{c}_2 t. \tag{51}$$

Then we can derive $V^{q-1}(s(t)) \le \frac{1}{\xi\bar{c}_2 t(q-1)}$. In addition, by defining $T_1 = \frac{1}{\xi\bar{c}_2(q-1)}$, it can be determined that $\forall t \ge T_1$, we have $V^{q-1}(s(t)) \le 1$ and $V(s(t)) \le 1$.

Situation 2 If $V(s) \le 1$, one has

$$\dot{V}(s) \le -\xi\underline{c}_1 V^p(s) - (1-\xi)\underline{c}_1 V^p(s) + \underline{b}_n. \tag{52}$$

Define $\Xi_s = \big\{s|V^p(s) \le \frac{\underline{b}_n}{(1-\xi)\underline{c}_1}\big\}$ and $\bar{\Xi}_s = \big\{s|V^p(s) > \frac{\underline{b}_n}{(1-\xi)\underline{c}_1}\big\}$.

1. If $s(t) \in \bar{\Xi}_s$, according to (52), we have

$$\dot{V}(s) \le -\xi\underline{c}_1 V^p(s), \tag{53}$$

which means

$$\int_{t_0}^t \frac{\dot{V}(s)}{V^p(s)}\mathrm{d}t \le -\xi\int_{t_0}^t \underline{c}_1\mathrm{d}t. \tag{54}$$

Computing (54) yields

$$\frac{1}{1-p}V^{1-p}(s(t)) - \frac{1}{1-p}V^{1-p}(s(t_0)) \le -\xi\underline{c}_1(t-t_0). \tag{55}$$

Based on Situation 1, we have $V(s(t_0)) \le 1$ for $t_0 \ge T_1$. Thus, it can be achieved that $V^{1-p}(s(t)) \le 1 - \xi\underline{c}_1(1-p)(t-t_0)$. By defining $T_2 \ge \frac{1}{\xi\underline{c}_1(1-p)}$ and considering the positive definite property of $V(s)$, we can obtain $V^p(s) \le \frac{\underline{b}_n}{\underline{c}_1(1-\xi)}$ $\forall t \ge t_0 + T_2$.

2. If $s(t) \in \Xi_s$, considering LaSalle's invariance principle, it is true that $s(t)$ does not violate the set Ξ_s. Based on the aforementioned analysis, because Ξ_s is an invariant set, we can find that $V^p(s) \le \frac{\underline{b}_n}{\underline{c}_1(1-\xi)}$ is true $\forall t \ge T_1 + T_2$. Moreover, in light of Lemma 1, we have $\|s\| \le \beta^{-1}(\frac{\underline{b}_n}{(1-\xi)\underline{c}_1})^{\frac{1}{p}}$. Therefore, the control system (1) can achieve stability in a fixed time, and the settling time T satisfies $T \le \frac{1}{\xi\underline{c}_1(1-p)} + \frac{1}{\xi\bar{c}_2(q-1)}$.

Furthermore, we prove that all states with constraints have not overstepped their constraints. Defining a parameter $P = \min\{\underline{c}_1, \bar{c}_2\}$ and combining Lemma 5, $\dot{V}_n$ can be simplified as

$$\dot{V}_n \le -PV_n + \underline{b}_n. \tag{56}$$

By multiplying both sides by e^{Pt} yields $\frac{\mathrm{d}(V_n\mathrm{e}^{Pt})}{\mathrm{d}t} \le \underline{b}_n\mathrm{e}^{Pt}$. Meanwhile, integrating both sides results in

$$V_n(t) \le V_n(0) + \frac{\underline{b}_n}{P}. \tag{57}$$

From Lemma 4 and inequality (57), the boundedness of $V_n(t)$ can be determined. According to the definition of $V_n(t)$, it can be found that e_i and $\tilde{\theta}$ are bounded. Note that $\alpha_{1,\mathrm{f}} \in L_\infty$ in compact set U_d and $e_1 = \zeta_1 - \alpha_{1,\mathrm{f}}$. It is guaranteed that $\zeta_1 \in L_\infty$. Thus, we can infer that state x_1 remains in interval U_1 formed by constraint functions $k_{1\mathrm{l}}(t)$ and $k_{1\mathrm{h}}(t)$ under the initial condition $x_1(0) \in U_1$, which means that x_1 does not overstep the time-varying asymmetric constraints. Similarly, the boundedness of ζ_i, $\alpha_{i,\mathrm{f}}$, and u can be obtained, while we can conclude that the constraint areas of system state x_i are not violated.

Finally, we will prove that the real tracking error $z = x_1 - y_\mathrm{d}$ is bounded. By calculation,

we can obtain $z=\frac{e_1}{\varrho}$, where $\varrho=\frac{\bar{k}_{1\mathrm{l}}-k_{1\mathrm{l}}}{(x_1-k_{1\mathrm{l}})(y_\mathrm{d}-k_{1\mathrm{l}})}+\frac{k_{1\mathrm{h}}-\underline{k}_{1\mathrm{h}}}{(k_{1\mathrm{h}}-x_1)(k_{1\mathrm{h}}-y_\mathrm{d})}$. Note that $x_1\in U_1$ and $y_\mathrm{d}\in U_\mathrm{d}\subset U_1$, which implies that there exist two positive constants $\bar{\nu}_j$ and $\underline{\nu}_j$ $(j=1,2)$, such that inequalities $0<\underline{\nu}_1\le(x_1-k_{1\mathrm{l}})(y_\mathrm{d}-k_{1\mathrm{l}})\le\bar{\nu}_1$ and $0<\underline{\nu}_2\le(k_{1\mathrm{h}}-x_1)(k_{1\mathrm{h}}-y_\mathrm{d})\le\bar{\nu}_2$ hold. This proves the boundedness of ϱ. Therefore, there exist two constants, $\underline{\varrho}$ and $\bar{\varrho}$, which satisfy $0<\underline{\varrho}\le\varrho\le\bar{\varrho}$, so z is bounded. Meanwhile, (56) can be rewritten as $\dot{V}_n(t)\le-Pe_1^2+\underline{b}_n$, which indicates that $\dot{V}_n(t)$ will be negative if $|e_1|>\sqrt{\frac{\underline{b}_n}{P}}$. Thus, it can be obtained that e_1 enters into and remains within the compact set $\Psi_{e1}=\left\{e_1\in\mathbb{R}||e_1|\le\sqrt{\frac{\underline{b}_n}{P}}\right\}$. In addition, we can find that the real tracking error z accesses the compact set and remains within the compact set $\Psi_z=\left\{z\in\mathbb{R}||z|\le\frac{1}{\underline{\varrho}}\sqrt{\frac{\underline{b}_n}{P}}\right\}$. Obviously, the tracking error can converge to a small range around zero in a predefined time by choosing an appropriate parameter P. The proof is completed.

4 Two examples

In this section, two examples are provided to verify the availability of the proposed control strategy.

4.1 Numerical example

In this subsection, the method presented in this paper would be compared with the BLF-based method in Li YX (2020). We take the following nonlinear system model into account:

$$\begin{cases}x_1=f_1(\bar{x}_2)+x_2,\\ x_2=f_2(\bar{x}_2)+g(\bar{x}_2)q(u),\\ y=x_1,\end{cases}\tag{58}$$

where $f_1(\bar{x}_2)=x_1^2x_2+0.1\cos(0.5x_1)$, $f_2(\bar{x}_2)=x_1+0.1x_2+0.5\sin x_2$, and $g(\bar{x}_2)=0.2\cos(x_1x_2)+1$. The desired signal is selected as $y_\mathrm{d}=\sin(0.5t)+0.5\cos t$, which satisfies Assumption 2. The system states are required to be maintained in the following areas:

$$\begin{aligned}x_i\in U_i:=\{(t,x_i)\in(\mathbb{R}_+\times\mathbb{R})|\\ k_{i\mathrm{l}}(t)<x_i<k_{i\mathrm{h}}(t),k_{i\mathrm{l}}\in\mathbb{R},k_{i\mathrm{h}}\in\mathbb{R}\},\end{aligned}\tag{59}$$

where $k_{1\mathrm{h}}(t)=-\sin t+\cos t+6$, $k_{1\mathrm{l}}(t)=0.5\sin t-6$, $k_{2\mathrm{h}}(t)=-0.2\sin t+0.4\cos t+6$, $k_{2\mathrm{l}}(t)=-\sin t+\cos t-6$. According to Theorem 1, the first-order filter, controllers, and adaptive law are constructed as (13), (35), and (38), respectively, and the virtual control signals are designed as (20) and (27). The related parameters are set to $c_{1,1}=c_{1,2}=c_{2,1}=c_{2,2}=2$, $k_1=k_2=70$, $a_1=a_2=5$, $\sigma_1=\sigma_2=\gamma=5$, $\tau_1=0.001$, $\bar{k}_{1\mathrm{h}}=\underline{k}_{1\mathrm{l}}=-2$, $\bar{k}_{2\mathrm{h}}=\underline{k}_{2\mathrm{l}}=-2$, $p=0.5$, $q=3$, $\lambda=0.3$, $u_{\min}=2$. The different parameters of the method in Li YX (2020) are set to $\sigma_1=10\mathrm{e}^{-2t}$, $\sigma_2=15\mathrm{e}^{-0.01t}$, $k_{a1}=k_{b1}=k_{a2}=k_{b2}=-2$, and the remaining parameters are the same as those in this work. The initial conditions are both selected as $x_1(0)=0.3$, $x_2(0)=0.2$, and $\theta(0)=2$.

The comparative results are shown in Figs. 3 and 4. Obviously, from Fig. 3, the UBF-based method proposed in this paper enables the system to obtain better tracking performance compared with the BLF-based method in Li YX (2020). The detailed comparisons are illustrated in Fig. 4. The tracking errors for the two methods are exhibited in Fig. 4a. In Figs. 4b and 4c, the differences in virtual control signals are demonstrated, where the virtual control signal can surpass the state constraints in Fig. 4b, but the system state still obeys the state constraints in Fig. 4d under the UBF-based method. In Fig. 4c, under the BLF-based method, the virtual control signal α_1 and the system state x_2 have not violated the state constraints.

The quantization input $q(u_i)$ and the system input u_i are displayed in Fig. 5a. The adaptive law is plotted in Fig. 5b.

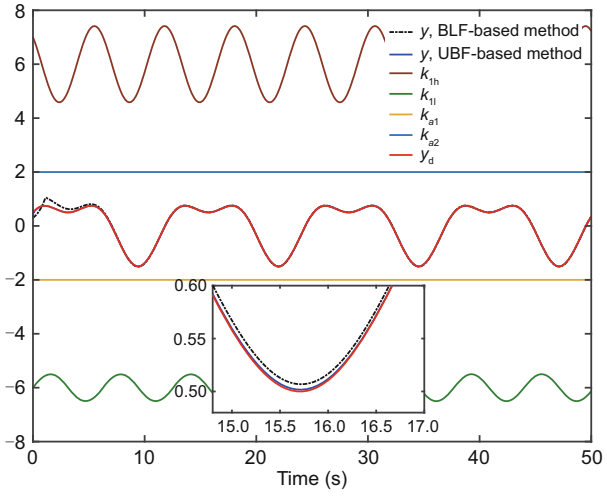

Fig. 3 Comparison of tracking trajectories after using the BLF-based method and UBF-based method (References to color refer to the online version of this figure)

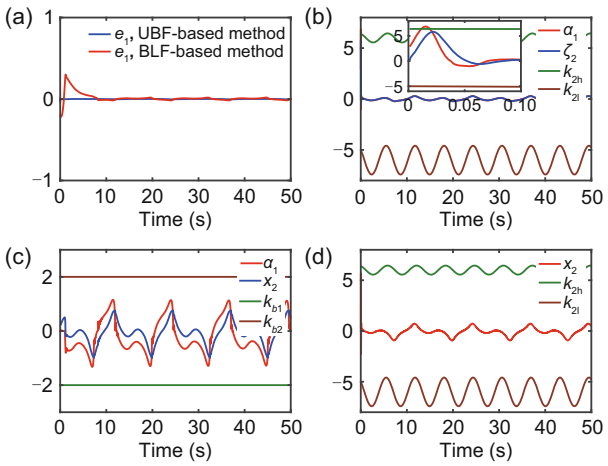

Fig. 4 Tracking errors of two methods (a), ζ_2 and α_1 under the UBF-based method (b), x_2 and α_1 under the BLF-based method (c), and x_2 under the UBF-based method (d) (References to color refer to the online version of this figure)

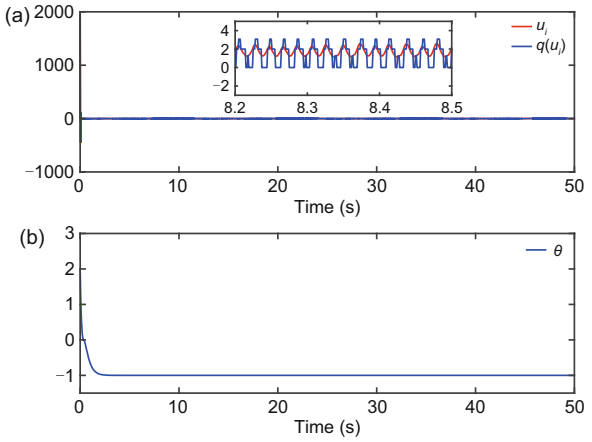

Fig. 5 $q(u_i)$ and u_i (a) and θ (b) for system (58) (References to color refer to the online version of this figure)

4.2 Practical example

In this subsection, we introduce a ship control problem described in Xing et al. (2017) as a practical example to illustrate the validity of the proposed method, which is modeled mathematically as follows:

$$\ddot{y} + \Phi\dot{y} + b_0(Mx_1^3 + Lx_1) = b_0 q(u_i), \tag{60}$$

where $b_0 \neq 0$ denotes a constant, $q(u_i)$ expresses the quantized input, and y represents the course angular velocity of the ship. L and M are unknown constants related to the hydrodynamic coefficients and the mass of the ship, respectively. By setting $x_1 = y$ and $x_2 = \dot{x}_1$, system (60) can be rewritten as

$$\begin{cases} \dot{x}_1 = x_2, \\ \dot{x}_2 = -\Phi x_2 - b_0(Mx_1^3 + Lx_1) + b_0 q(u_i). \end{cases} \tag{61}$$

Let $\Phi = -0.1$, $b_0 = 1$, $M = 0.7$, $L = 0.4$. Then we can derive $f_1(x_1, x_2) = 0$, $f_2(x_1, x_2) = -0.1x_2 - 0.4x_1 - 0.7x_1^2$, and $g(x_1, x_2) = 1$. The upper and lower bound functions of states x_1 and x_2 are set as $k_{1\mathrm{h}} = 0.5\sin t + 5$, $k_{2\mathrm{h}} = -\sin t + \cos t + 5$ and $k_{1\mathrm{l}} = -\sin t + \cos t - 5$, $k_{2\mathrm{l}} = -0.2\sin t + 0.4\cos t - 5$, respectively. Meanwhile, some relevant parameter values are chosen as $a_2 = 10$, $k_1 = 60$, $k_2 = 60$, $c_{11} = 5$, $c_{12} = 5$, $c_{21} = 15$, $c_{22} = 15$, $\gamma = 10$, $\sigma_1 = 5$, $\sigma_2 = 5$, $\delta = 0.05$, $\lambda = 0.1$, $u_{\min} = 2$, $\underline{k}_{1\mathrm{h}} = 2$, $\underline{k}_{2\mathrm{h}} = 2$, $\bar{k}_{1\mathrm{l}} = -2$, $\bar{k}_{2\mathrm{l}} = -2$, $\tau = 0.25$. The initial values of the controlled systems are selected as $x_1(0) = 0$, $x_2(0) = 0.3$, and $\theta(0) = 2$. The desired trajectories are provided by $y_{\mathrm{d}}(t) = \sin(0.5t)$.

Figs. 6 and 7 provide the simulation results. The tracking performance is shown in Fig. 6a and the tracking errors are given in Fig. 6c. The system states are exhibited in Figs. 6b and 6d, where the system states x_1 and x_2 have not overstepped their state constraints. Fig. 7a shows the quantized input and the input signal. The trajectory of the adaptive law is exhibited in Fig. 7b.

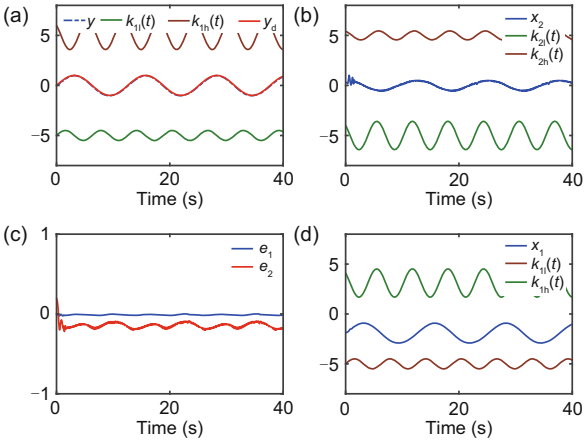

Fig. 6 Tracking trajectories (a), x_2 and its constraint functions (b), tracking errors (c), and x_1 and its constraint functions (d) for system (61) (References to color refer to the online version of this figure)

5 Conclusions

In this paper, we researched the issue of adaptive tracking control for a class of uncertain nonlinear

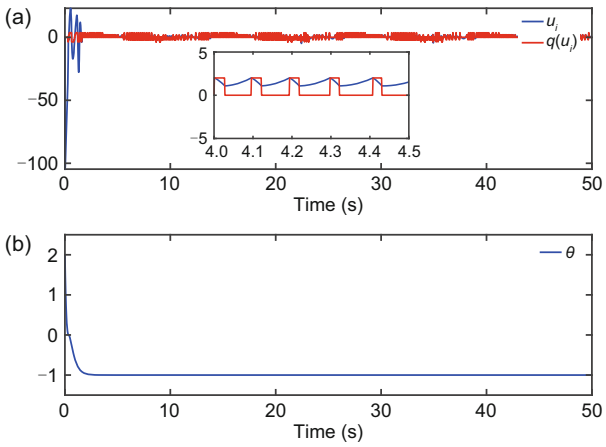

Fig. 7 $q(u_i)$ and u_i (a) and θ (b) for system (61) (References to color refer to the online version of this figure)

systems with input quantization and time-varying asymmetric constraints. Based on the UBF method, a practical fixed-time adaptive fuzzy control strategy has been developed which guarantees that the time-varying asymmetric state constraints are not overstepped and removes the feasibility condition of virtual control signals. By introducing the command filter method, the "explosion of complexity" issue has been addressed. FLSs have been applied to approximate unknown nonlinear functions. According to the practical fixed-time Lyapunov stability criterion, it has been demonstrated that the tracking error will converge to an expected range around zero in a predetermined time. The effectiveness of the proposed strategy is illuminated using two simulation examples.

Contributors

Ben NIU supervised the project. Zixuan HUANG performed numerical simulations. Adil M. AHMAD accomplished experimental verification. Zixuan HUANG drafted the paper. Huanqing WANG helped organize the paper. Xudong ZHAO revised and finalized the paper.

Acknowledgements

The authors gratefully acknowledge the technical and financial support provided by the Ministry of Education and King Abdulaziz University, DSR, Jeddah, Saudi Arabia.

Conflict of interest

All the authors declare that they have no conflict of interest.

Data availability

The data that support the findings of this study are available from the corresponding author upon reasonable request.

References

Bhat SP, Bernstein DS, 1998. Continuous finite-time stabilization of the translational and rotational double integrators. *IEEE Trans Autom Contr*, 43(5):678-682. https://doi.org/10.1109/9.668834

Chen B, Liu XP, Liu KF, et al., 2013. Adaptive fuzzy tracking control of nonlinear MIMO systems with time-varying delays. *Fuzzy Sets Syst*, 217:1-21. https://doi.org/10.1016/j.fss.2012.11.002

Chen WS, Li JM, 2010. Globally decentralized adaptive backstepping neural network tracking control for unknown nonlinear interconnected systems. *Asian J Contr*, 12(1):96-102. https://doi.org/10.1002/asjc.160

Gao ZF, Liu DH, Qian MS, 2022. Decentralised adaptive tracking control for the interconnected nonlinear systems with asymmetric full state dynamic constraints. *Int J Contr*, 95(10):2840-2853. https://doi.org/10.1080/00207179.2021.1939421

Guo SY, Zhao XD, Wang HQ, et al., 2023. Distributed consensus of heterogeneous switched nonlinear multiagent systems with input quantization and DoS attacks. *Appl Math Comput*, 456:128127. https://doi.org/10.1016/j.amc.2023.128127

Hou HZ, Yu XH, Xu L, et al., 2020. Finite-time continuous terminal sliding mode control of servo motor systems. *IEEE Trans Ind Electron*, 67(7):5647-5656. https://doi.org/10.1109/TIE.2019.2931517

Huang JS, Wang W, Wen CY, et al., 2018. Adaptive control of a class of strict-feedback time-varying nonlinear systems with unknown control coefficients. *Automatica*, 93:98-105. https://doi.org/10.1016/j.automatica.2018.03.061

Huang S, Zong GD, Wang HQ, et al., 2023. Command filter-based adaptive fuzzy self-triggered control for MIMO nonlinear systems with time-varying full-state constraints. *Int J Fuzzy Syst*, 25:3144-3161. https://doi.org/10.1007/s40815-023-01560-8

Kim BS, Yoo SJ, 2015. Adaptive control of nonlinear pure-feedback systems with output constraints: integral barrier Lyapunov functional approach. *Int J Contr Autom Syst*, 13(1):249-256. https://doi.org/10.1007/s12555-014-0018-3

Li JP, Yang YN, Hua CC, et al., 2017. Fixed-time backstepping control design for high-order strict-feedback non-linear systems via terminal sliding mode. *IET Contr Theory Appl*, 11(8):1184-1193. https://doi.org/10.1049/iet-cta.2016.1143

Li SH, Wang XY, 2013. Finite-time consensus and collision avoidance control algorithms for multiple AUVs. *Automatica*, 49(11):3359-3367. https://doi.org/10.1016/j.automatica.2013.08.003

Li YM, Tong SC, 2017. Adaptive fuzzy output constrained control design for multi-input multi-output stochastic nonstrict-feedback nonlinear systems. *IEEE Trans Cybern*, 47(12):4086-4095. https://doi.org/10.1109/TCYB.2016.2600263

Li YX, 2019. Finite time command filtered adaptive fault tolerant control for a class of uncertain nonlinear systems. *Automatica*, 106:117-123. https://doi.org/10.1016/j.automatica.2019.04.022

Li YX, 2020. Barrier Lyapunov function-based adaptive asymptotic tracking of nonlinear systems with unknown virtual control coefficients. *Automatica*, 121:109181. https://doi.org/10.1016/j.automatica.2020.109181

Liu SL, Niu B, Zong GD, et al., 2024. Adaptive neural dynamic-memory event-triggered control of high-order random nonlinear systems with deferred output constraints. *IEEE Trans Autom Sci Eng*, 21(3):2779-2791. https://doi.org/10.1109/TASE.2023.3269509

Liu YJ, Tong SC, 2017. Barrier Lyapunov functions for Nussbaum gain adaptive control of full state constrained nonlinear systems. *Automatica*, 76:143-152. https://doi.org/10.1016/j.automatica.2016.10.011

Ma H, Liang HJ, Zhou Q, et al., 2019. Adaptive dynamic surface control design for uncertain nonlinear strict-feedback systems with unknown control direction and disturbances. *IEEE Trans Syst Man Cybern Syst*, 49(3):506-515. https://doi.org/10.1109/TSMC.2018.2855170

Ni JK, Liu L, Liu CX, et al., 2017. Fast fixed-time nonsingular terminal sliding mode control and its application to chaos suppression in power system. *IEEE Trans Circ Syst II Expr Briefs*, 64(2):151-155. https://doi.org/10.1109/TCSII.2016.2551539

Polyakov A, 2012. Nonlinear feedback design for fixed-time stabilization of linear control systems. *IEEE Trans Autom Contr*, 57(8):2106-2110. https://doi.org/10.1109/TAC.2011.2179869

Shi Y, Shao XL, Zhang WD, 2020. Quantized learning control for flexible air-breathing hypersonic vehicle with limited actuator bandwidth and prescribed performance. *Aerosp Sci Technol*, 97:105629. https://doi.org/10.1016/j.ast.2019.105629

Sui S, Tong SC, 2018. Observer-based adaptive fuzzy quantized tracking DSC design for MIMO nonstrict-feedback nonlinear systems. *Neur Comput Appl*, 30(11):3409-3419. https://doi.org/10.1007/s00521-017-2929-4

Sun ZY, Liu CY, Su SF, et al., 2021. Robust stabilization of high-order nonlinear systems with unknown sensitivities and applications in humanoid robot manipulation. *IEEE Trans Syst Man Cybern Syst*, 51(7):4409-4416. https://doi.org/10.1109/TSMC.2019.2931768

Swaroop D, Hedrick JK, Yip PP, et al., 2000. Dynamic surface control for a class of nonlinear systems. *IEEE Trans Autom Contr*, 45(10):1893-1899. https://doi.org/10.1109/TAC.2000.880994

Tang ZL, Ge SS, Tee KP, et al., 2016. Robust adaptive neural tracking control for a class of perturbed uncertain nonlinear systems with state constraints. *IEEE Trans Syst Man Cybern Syst*, 46(12):1618-1629. https://doi.org/10.1109/TSMC.2015.2508962

Tee KP, Ge SS, 2011. Control of nonlinear systems with partial state constraints using a barrier Lyapunov function. *Int J Contr*, 84(12):2008-2023. https://doi.org/10.1080/00207179.2011.631192

Tee KP, Ge SS, Tay EH, 2009. Barrier Lyapunov functions for the control of output-constrained nonlinear systems. *Automatica*, 45(4):918-927. https://doi.org/10.1016/j.automatica.2008.11.017

Wang F, Lai GY, 2020. Fixed-time control design for nonlinear uncertain systems via adaptive method. *Syst Contr Lett*, 140:104704. https://doi.org/10.1016/j.sysconle.2020.104704

Wang HQ, Chen B, Liu XP, et al., 2013. Robust adaptive fuzzy tracking control for pure-feedback stochastic nonlinear systems with input constraints. *IEEE Trans Cybern*, 43(6):2093-2104. https://doi.org/10.1109/TCYB.2013.2240296

Wang SX, Xia JW, Park JH, et al., 2021. Adaptive event-triggered control for MIMO nonlinear systems with asymmetric state constraints based on unified barrier functions. *Int J Rob Nonl Contr*, 31(18):9397-9415. https://doi.org/10.1002/rnc.5776

Wang T, Zhang YF, Qiu JB, et al., 2015. Adaptive fuzzy backstepping control for a class of nonlinear systems with sampled and delayed measurements. *IEEE Trans Fuzzy Syst*, 23(2):302-312. https://doi.org/10.1109/TFUZZ.2014.2312026

Xing LT, Wen CY, Liu ZT, et al., 2017. Robust adaptive output feedback control for uncertain nonlinear systems with quantized input. *Int J Rob Nonl Contr*, 27(11):1999-2016. https://doi.org/10.1002/rnc.3669

Xu B, Liang YJ, Li YX, et al., 2022. Adaptive command filtered fixed-time control of nonlinear systems with input quantization. *Appl Math Comput*, 427:127186. https://doi.org/10.1016/j.amc.2022.127186

Yang HJ, Shi P, Zhao XD, et al., 2016. Adaptive output-feedback neural tracking control for a class of nonstrict-feedback nonlinear systems. *Inform Sci*, 334-335:205-218. https://doi.org/10.1016/j.ins.2015.11.034

Yu S, Yu X, Shirinzadeh B, et al., 2005. Continuous finite-time control for robotic manipulators with terminal sliding mode. *Automatica*, 41(11):1957-1964. https://doi.org/10.1016/j.automatica.2005.07.001

Zhang LC, Liang HJ, Sun Y, et al., 2021. Adaptive event-triggered fault detection scheme for semi-Markovian jump systems with output quantization. *IEEE Trans Syst Man Cybern Syst*, 51(4):2370-2381. https://doi.org/10.1109/TSMC.2019.2912846

Zhao H, Wang HQ, Xu N, et al., 2023. Fuzzy approximation-based optimal consensus control for nonlinear multi-agent systems via adaptive dynamic programming. *Neurocomputing*, 553:126529. https://doi.org/10.1016/j.neucom.2023.126529

Zhao K, Song YD, Chen CLP, et al., 2020. Control of nonlinear systems under dynamic constraints: a unified barrier function-based approach. *Automatica*, 119:109102. https://doi.org/10.1016/j.automatica.2020.109102

Zuo ZY, Tian BL, Defoort M, et al., 2018. Fixed-time consensus tracking for multiagent systems with high-order integrator dynamics. *IEEE Trans Autom Contr*, 63(2):563-570. https://doi.org/10.1109/TAC.2017.2729502